

Quantum Monte Carlo simulation of overpressurized liquid ^4He

L. Vranješ

Faculty of Natural Sciences, University of Split, 21000 Split, Croatia

J. Boronat, J. Casulleras, and C. Cazorla

*Departament de Física i Enginyeria Nuclear, Campus Nord B4-B5,
Universitat Politècnica de Catalunya, E-08034 Barcelona, Spain*

(Dated: March 23, 2022)

A diffusion Monte Carlo simulation of superfluid ^4He at zero temperature and pressures up to 275 bar is presented. Increasing the pressure beyond freezing (~ 25 bar), the liquid enters the overpressurized phase in a metastable state. In this regime, we report results of the equation of state and the pressure dependence of the static structure factor, the condensate fraction, and the excited-state energy corresponding to the roton. Along this large pressure range, both the condensate fraction and the roton energy decrease but do not become zero. The roton energies obtained are compared with recent experimental data in the overpressurized regime.

PACS numbers: 67.40.-w, 67.80.-s

Quantum fluids in metastable states are presently a research topic of fundamental interest from both the experimental and theoretical viewpoints [1]. The extremely low temperature achieved in liquid helium makes this liquid the most pure in nature and therefore the optimal choice for observing homogeneous nucleation, which is an intrinsic property of the liquid. Caupin, Balibar and collaborators have studied profusely the negative pressure regime by focusing high intensity ultrasound bursts in bulk helium [2, 3]. In liquid ^4He they have measured a negative pressure of -9.4 bar, only 0.2 bar above the spinodal point predicted by microscopic theory [4, 5]. The same experimental team has used recently this acoustic technique to pressurize small quantities of liquid ^4He up to 160 bar at temperatures $0.05 \text{ K} < T < 1 \text{ K}$ [6]. This pressure is the highest pressure ever realized in overpressurized liquid ^4He and is much larger than the liquid-solid equilibrium pressure, which at $T = 0 \text{ K}$ is 25.3 bar. In the experimental setup used by Werner *et al.* [6], the overpressurized regime has become accessible by avoiding nucleation on the walls of the container and therefore allowing only homogeneous nucleation. This nucleation was not observed along this large increase of the liquid pressure beyond the freezing point.

Liquid ^4He in metastable states has also been obtained by immersing it in different porous media. Albergamo *et al.* [7] have carried out neutron scattering experiments in a medium with 47 Å pore diameter filled with densities below the equilibrium density and negative pressures up to -5 bar. The achievement of negative pressures in this medium is attributed to the stretching that the liquid supports due to the strong attraction to the walls. Using a different material, with 44 Å pore diameter, Pearce *et al.* [8] have reported neutron scattering data in the high density regime observing a liquid phase up to ~ 40 bar. Therefore, the confinement of helium in porous media makes feasible extensions of the pressure

on both sides of the stable liquid phase. The nature of these two metastable regions presents a significant difference. At negative pressure, there exists an end point (spinodal point) where the speed of sound becomes zero, and it is thermodynamically forbidden to cross it maintaining a homogeneous liquid phase. On the contrary, such a point does not exist on the overpressurized side. Nevertheless, Schneider and Enz [9] suggested that the pressurized phase has also an end point corresponding to the pressure where the excitation energy of the roton might vanish. On the other hand, and according to Jackson *et al.* [10] and Halinen *et al.* [11], the vanishing of the roton energy is not the instability that causes the liquid-solid transition in ^4He but another one involving a 6-fold symmetric soft mode in the two-body correlations.

The roton mode is not observed anymore when liquid ^4He crystallizes. In the overpressurized regime, between 25 and 38.5 bar, the neutron-scattering data of Ref. [8] show the roton excitation, while the maxon disappears, probably due to the fact that its corresponding energy might exceed twice the roton energy. At the liquid-solid transition, the roton energy is still finite. The latter feature means that ^4He is superfluid when it crystallizes. This result seems to be in disagreement with a recent experimental work by Yamamoto *et al.* [12] who reported a critical temperature $T_c = 0$ at a pressure $P \sim 35$ bar in a porous material. As a first explanation, the differences observed in the two experiments can be attributed to the smaller pore diameter (25 Å) used by Yamamoto *et al.* [12], but additional work would be necessary to confirm this argument. It is worth noticing that the findings of Ref. [12] imply the existence of a superfluid to normal phase transition at zero temperature, an intriguing possibility that makes the overpressurized regime even more interesting. In this direction, Nozières [13] has predicted recently that the condensate fraction could vanish at a certain pressure, and therefore a normal liquid before

freezing would be possible.

At present, the theoretical knowledge of the metastable regime at negative pressures is rather complete with an overall agreement among quantum Monte Carlo, hypernetted chain (HNC) based on Euler-Lagrange optimization, and density functional approaches [1]. On the contrary, the pressurized liquid remains until now nearly unexplored. In the present work, we present diffusion Monte Carlo (DMC) results for the overpressurized phase up to $P \sim 275$ bar. The DMC method is probably the best suited way to deal with this metastable regime since the physical phase of the system is controlled by the trial wave function used for importance sampling. Our results show a superfluid phase in which, up to the highest pressure studied, the condensate fraction is small but discernible and the excitation energy of the roton decreases but does not reach the zero limit.

The DMC method is nowadays a well-known tool devised to study quantum fluids and solids at zero temperature. Its starting point is the Schrödinger equation written in imaginary time,

$$-\hbar \frac{\partial \Psi(\mathbf{R}, t)}{\partial t} = (H - E_r) \Psi(\mathbf{R}, t), \quad (1)$$

with an N -particle Hamiltonian

$$H = -\frac{\hbar^2}{2m} \sum_{i=1}^N \nabla_i^2 + \sum_{i<j}^N V(r_{ij}). \quad (2)$$

In Eq. (1), E_r is a constant acting as a reference energy and $\mathbf{R} \equiv (\mathbf{r}_1, \dots, \mathbf{r}_N)$ is a *walker* in Monte Carlo terminology. DMC solves stochastically the Schrödinger equation (1) replacing $\Psi(\mathbf{R}, t)$ by $\Phi(\mathbf{R}, t) = \Psi(\mathbf{R}, t)\psi(\mathbf{R})$ with $\psi(\mathbf{R})$ a trial wave function used for importance sampling. When $t \rightarrow \infty$ only the lowest energy eigenfunction, not orthogonal to $\psi(\mathbf{R})$, survives. The simulation of the liquid in its ground state is carried out by using a Jastrow approximation, $\psi_J(\mathbf{R}) = \prod_{i<j}^N f(r_{ij})$. As in our previous work [14] on the equation of state of liquid ^4He in the stable regime, $f(r)$ is a model proposed by Reatto [15] which incorporates nearly optimal short and medium range two-body correlations. As a matter of comparison, simulations of the crystalline hcp phase have been also carried out; in this case, a Nosanow-Jastrow model is used, $\psi_{\text{NJ}}(\mathbf{R}) = \psi_J(\mathbf{R}) \prod_i^N g(r_{iI})$, with $g(r)$ a gaussian function linking every particle i to a fixed point \mathbf{r}_I of the lattice.

The calculation of the roton energy using the DMC method is more involved since it corresponds to an excited state. In this case, we have taken as a trial wave function for importance sampling an eigenstate of the total momentum operator which incorporates backflow correlations, as originally proposed by Feynman and Cohen [16],

$$\psi_{\text{BF}}(\mathbf{R}) = \sum_{i=1}^N e^{i\mathbf{q} \cdot \tilde{\mathbf{r}}_i} \psi_J(\mathbf{R}), \quad (3)$$

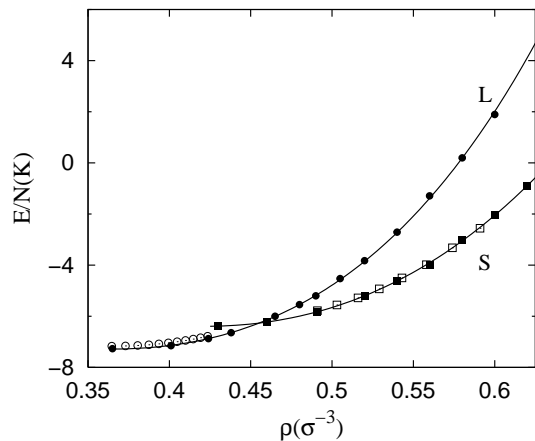


FIG. 1: Energy per particle of liquid ^4He from the equilibrium density up to the highest density calculated, $0.6 \sigma^{-3}$, (solid circles). The solid line corresponds to the fit to the DMC energies using Eq. (4), and the open circles are experimental data in the stable regime from Ref. [18]. DMC results for the solid phase are shown as solid squares and compared with experimental data from Ref. [19] (open squares). The error bars of our data are smaller than the size of the symbols.

with $\tilde{\mathbf{r}}_i = \mathbf{r}_i + \sum_{j \neq i}^N \eta(r_{ij}) \mathbf{r}_{ij}$, and $\eta(r) = \lambda \exp[-((r - r_b)/\omega_b)^2]$. The only objective of our calculation is the energy of the collective mode, which is the same for excitations with momenta \mathbf{q} and $-\mathbf{q}$. Therefore, we avoid the complexity of working with a complex wave function (3) by using a superposition of both states. Proceeding in this form, the excited state turns into a fermion-like problem since the trial wave function is real but not positive everywhere [17]. In a first step, we have used the fixed-node (FN) approximation, which provides an upper bound to the roton energy. We verified that the introduction of backflow correlations in the trial wave function produces results quite close to experimental data at the equilibrium density, especially near the roton minimum. The nodal constraint imposed by FN is removed, in a second step, by using the released-node (RN) technique in which the walkers are allowed to cross the nodal surface imposed by ψ and survive for a finite lifetime.

In Fig. 1, we report the results obtained for the energy per particle of the liquid phase as a function of the density. The He-He interaction corresponds to the HFD-B(HE) Aziz potential [20] and the number of atoms used in the simulation increases with density: $N = 150$ near freezing and $N = 250$ at the highest densities; periodic boundary conditions are assumed in all the simulations. Possible biases coming from the use of a finite number of walkers and from a finite time-step in the employed second-order algorithm are reduced to the level of the statistical noise. The DMC energies are accurately parameterized, from the spinodal point up to the highest

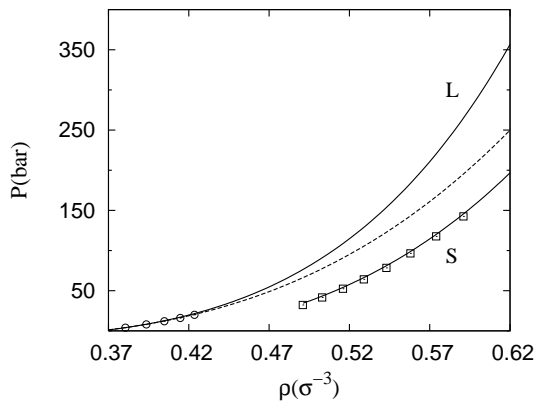


FIG. 2: Pressure as a function of the density. The solid lines stand for the DMC results obtained from the equations of state of the liquid and solid phases shown in Fig. 1. The dashed line is the extrapolation from experimental data [6, 22]; the symbols correspond to experimental data for the liquid [18] and solid phases [19].

densities calculated, by the analytical form

$$e(\rho) = e_0 + e_1(\rho/\rho_c - 1)(1 - (\rho/\rho_c - 1)) + b_3(\rho/\rho_c - 1)^3 + b_4(\rho/\rho_c - 1)^4, \quad (4)$$

with $e = E/N$, and $\rho_c = 0.264 \sigma^{-3}$ ($\sigma = 2.556 \text{ \AA}$) the spinodal density. The rest of parameters in Eq. (4) are $e_0 = -6.3884(40) \text{ K}$, $e_1 = -4.274(31) \text{ K}$, $b_3 = 1.532(12) \text{ K}$, and $b_4 = 1.433(24) \text{ K}$, the figures in parenthesis being the statistical errors [21]. DMC results of the energies of the solid phase, calculated using the Nosanow-Jastrow trial wave function and an hcp lattice, are also shown in Fig. 1. The comparison between the liquid and solid phase simulations shows clearly that DMC is effectively able to study the overpressurized liquid phase in spite of not being the ground-state (minimum energy) configuration, which manifestly corresponds to the solid phase beyond the freezing point.

Using the equation of state (4), the pressure is obtained from its thermodynamic definition $P(\rho) = \rho^2(\partial e/\partial \rho)$. The results obtained, which are shown in Fig. 2, reproduce accurately the experimental data [18] in the stable regime and predict a pressure $P \simeq 275 \text{ bar}$ at the highest density evaluated, $\rho = 0.6 \sigma^{-3}$. Our results are compared in the same figure with the analytic form suggested in Ref. [6], adjusted to Abraham's experimental data [22]. Below the freezing point, both curves agree but they give significantly different values at higher densities; the difference amounts to $\sim 100 \text{ bar}$ at $\rho = 0.6 \sigma^{-3}$. As a matter of comparison, the figure also shows the pressure of the solid phase, derived from the DMC equation of state shown in Fig. 1.

A characteristic feature of a solid phase is the presence of high-intensity peaks in the static structure function $S(q) = \langle \rho_{\mathbf{q}} \rho_{-\mathbf{q}} \rangle / N$, $\rho_{\mathbf{q}} = \sum_{i=1}^N e^{i\mathbf{q} \cdot \mathbf{r}_i}$, in the reciprocal lattice sites. Following the overpressurized liquid phase,

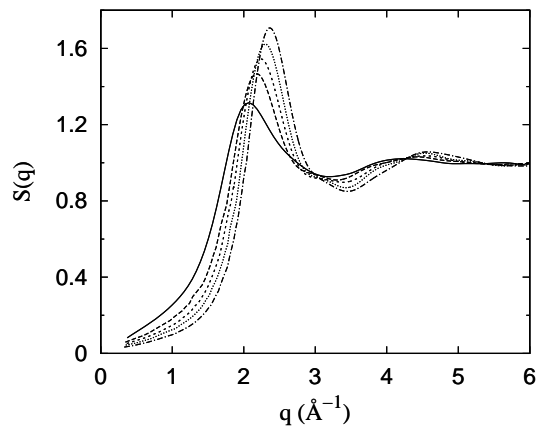


FIG. 3: Static structure function of the liquid phase for different densities. From bottom to top in the height of the main peak, the results correspond to densities 0.365 , 0.438 , 0.490 , 0.540 , and $0.6 \sigma^{-3}$.

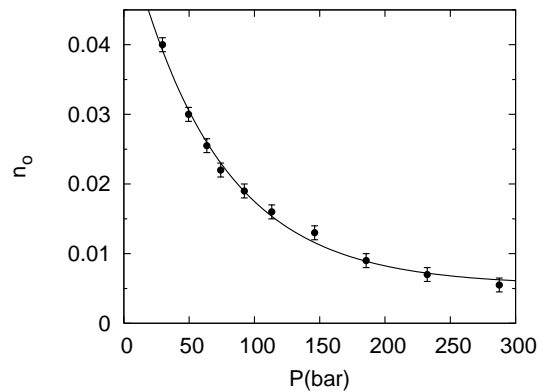


FIG. 4: Condensate fraction of liquid ^4He in the overpressurized regime. The line is an exponential fit to the DMC results.

we have not observed this feature and thus the liquid nature of the system is confirmed. In Fig. 3, results of $S(q)$ for densities ranging from equilibrium up to the highest densities studied are reported. The results show the expected behavior: when ρ increases, the strength of the main peak increases and moves to higher momenta in a monotonic way. At low momenta, the slope of $S(q)$ decreases with the density, following the limiting behavior $\lim_{q \rightarrow 0} S(q) = \hbar q / (2mc)$ driven by the speed of sound c .

A characteristic signature of bulk superfluid ^4He is a finite value of its condensate fraction, i.e., the fraction of particles occupying the zero-momentum state. As usual in a homogeneous system, the condensate fraction n_0 has been estimated from the long range behavior of the one-body density matrix, $\lim_{r \rightarrow \infty} \rho(r) = n_0$. The results obtained for n_0 , from the melting pressure up to nearly 300 bar , are plotted in Fig. 4. The line on top of the data corresponds to an exponential fit which reproduces quite accurately our DMC results ($n_0(P) \simeq A e^{-\beta P}$, with $A = 0.052$ and $\beta = 0.015 \text{ bar}^{-1}$). As one can see in

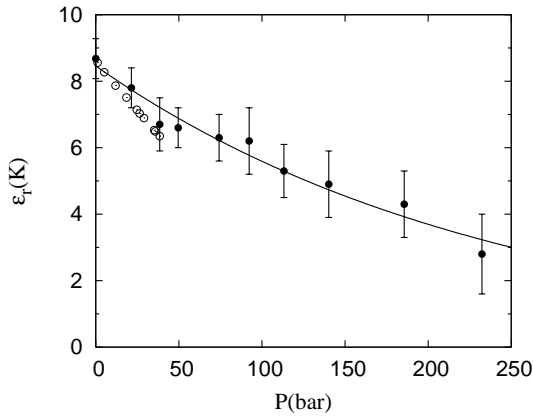


FIG. 5: Roton energy as a function of the density (solid circles). Open circles stand for experimental data from Ref. [8]. The line is an exponential fit to the DMC data.

the figure, n_0 decreases quite fast until $P = 100$ bar and then the slope decreases, approaching a value $n_0 \simeq 0.005$ at the highest density. With the same procedure, we obtained [14] $n_0 = 0.084(1)$ at the equilibrium density $\rho_0 = 0.365 \sigma^{-3}$, value which is compatible with PIMC estimations at low temperature [23] ($0.069(10)$ at $T = 1.18$ K and $0.087(10)$ at $T = 1.54$ K).

Superfluidity in bulk ^4He is manifested in the dynamic structure function by the clear signature of the roton collective mode. By increasing the density the roton energy ϵ_r decreases, and its approach to zero has been proposed as a possible final point in the overpressurized regime [9]. Trying to discern this hypothesis, we have carried out a RN calculation of the roton energy beyond the freezing point. The same methodology was used in the past in a DMC calculation of the phonon-roton spectrum at equilibrium and freezing densities [17] arriving at an accurate description of the experimental data. The results obtained are shown in Fig. 5. Experimental data obtained by neutron scattering experiments on superfluid ^4He in a porous media and up to 40 bar are also plotted in the figure [8]. From 0 to 40 bar, ϵ_r decreases linearly with the pressure and our data reproduces well this behavior. However, increasing the pressure this slope is reduced and, at the highest density studied the roton energy is still different from zero ($\epsilon_r = 2.8 \pm 1.2$ K at $\rho = 0.58 \sigma^{-3}$). It is worth noticing that the statistical errors are rather large and difficult to reduce since $\epsilon_r = E_r - E_0$, with E_r and E_0 the total energy of the excited and ground state, respectively. The excited state energy is estimated through an exponential fit $E(t) = E_r + Ae^{-(t/\tau)}$, with t the released time. The uncertainty of this extrapolation is under control since in all cases the difference between considering the last calculated point in released time or E_r is of the same order as the statistical noise. At each density, the number of particles has been adjusted to be as close to the roton momentum as possible; neverthe-

less, as only discrete values of q are accessible, possible corrections to the energy due to this fact are estimated to be less than 0.5 K in all cases. The obtained values of the roton momentum do not follow linear dependence with pressure, as the data in the stable liquid regime might suggest [24]. As the pressure is increased, the slope of the roton momentum as a function of pressure decreases.

In summary, the present DMC study of superfluid ^4He in the overpressurized regime does not show any signature of final (spinodal) point. The structure factor, condensate fraction, and roton energy are mainly driven by the density and not by the pressure. As shown in Figs. 1 and 2, equal changes in density in the stable and metastable regimes produce different changes in pressure. This leads, in the density range studied, to an approximated exponential behavior with pressure of magnitudes like n_0 and ϵ_r .

We thank M. Barranco, F. Caupin, J. Navarro, and M. Saarela for useful discussions. Partial financial support from DGI (Spain) Grant No. BFM2002-00466 and Generalitat de Catalunya Grant No. 2001SGR-00222 is gratefully acknowledged. We acknowledge the support of Central Computing Services at the Johannes Kepler University in Linz, where part of the computations were performed.

-
- [1] *Liquids Under Negative Pressures*, edited by A. R. Imre *et al.* (Kluwer Ac. Publishers, Dordrecht, 2002).
 - [2] F. Caupin and S. Balibar, Phys. Rev. B **64**, 064507 (2001).
 - [3] S. Balibar, J. Low Temp. Phys. **129**, 363 (2002).
 - [4] J. Boronat *et al.*, Phys. Rev. B **50**, 3427 (1994).
 - [5] G. H. Bauer *et al.*, Phys. Rev. B **61**, 9055 (2000).
 - [6] F. Werner *et al.*, J. Low. Temp. Phys. **136**, 93 (2004).
 - [7] F. Albergamo *et al.*, Phys. Rev. Lett. **92**, 235301 (2004).
 - [8] J. V. Pearce *et al.*, Phys. Rev. Lett. **93**, 145303 (2004).
 - [9] T. Schneider and C. P. Enz, Phys. Rev. Lett. **125**, 1186 (1971).
 - [10] A. D. Jackson *et al.*, Phys. Rev. B **24**, 105 (1981).
 - [11] J. Halinen *et al.*, J. Low Temp. Phys. **121**, 531 (2000).
 - [12] K. Yamamoto *et al.*, Phys. Rev. Lett. **93**, 075302 (2004).
 - [13] P. Nozières, J. Low Temp. Phys. **137**, 45 (2004).
 - [14] J. Boronat and J. Casulleras, Phys. Rev. B **49**, 8920 (1994).
 - [15] L. Reatto, Nucl. Phys. **A328**, 253 (1979).
 - [16] R. P. Feynman and M. Cohen, Phys. Rev. **102**, 1189 (1956).
 - [17] J. Boronat and J. Casulleras, Europhys. Lett. **38**, 291 (1997).
 - [18] R. De Bruyn Ouboter and C. N. Yang, Physica B **44**, 127 (1987).
 - [19] D. O. Edwards and R. C. Pandorff, Phys. Rev. **140**, 816 (1965).
 - [20] R. A. Aziz *et al.*, Mol. Phys. **61**, 1487 (1987).
 - [21] Partial results were presented in Quantum Fluids and Solids'04 and appear in its Proceedings (L. Vranješ *et al.*, J. Low Temp. Phys. **138**, 43 (2005)).

- [22] B. Abraham *et al.*, Phys. Rev. A **1**, 250 (1970).
- [23] D. M. Ceperley and E. L. Pollock, Can. J. Phys. **65**, 1416 (1987).
- [24] M. R. Gibbs *et al.*, J. Phys.: Condens. Matter **11**, 603 (1999).